

30. TURONIAN–SANTONIAN BENTHIC FORAMINIFER ASSEMBLAGES FROM SITE 959D (CÔTE D'IVOIRE-GHANA TRANSFORM MARGIN, EQUATORIAL ATLANTIC): INDICATION OF A LATE CRETACEOUS OXYGEN MINIMUM ZONE¹

Ann E.L. Holbourn^{2,3} and Wolfgang Kuhnt²

ABSTRACT

Turonian–Santonian organic-rich fissile black claystones with laminated intervals from Hole 959D on the Côte d'Ivoire-Ghana Transform Margin, drilled during Ocean Drilling Program Leg 159, contain benthic foraminifer assemblages dominated by buliminid associations. The lower Turonian assemblage from Core 159-959D-68R is strongly dominated by *Bolivina anambra*, *Praebulimina* sp. 1, *Praebulimina* sp. 2, *Praebulimina* sp. 3, and *Gavelinella* spp. The upper Turonian to lower Coniacian assemblage from Core 159-959D-67R displays low abundance and low diversity and consists mostly of organically cemented agglutinated taxa and/or some corroded tests of *Lenticulina*, *Bolivina*, *Gyroidinoides* ex gr. *nitidus*. The middle Coniacian to lower Santonian assemblage from Core 159-959D-66R and from the base of Core 159-959D-65R contains high numbers of *Praebulimina robusta*, *Praebulimina jang*, *Neobulimina subregularis*, and *Buliminella* cf. *gabonica*, but shows marked fluctuations in abundance and diversity, which appear to be related to changes in total organic carbon. The distinct composition of the two buliminid associations in Core 159-959D-68R and Core 159-959D-66R suggests that endemism was stronger during the early Turonian, when circulation was probably more restricted and connections between equatorial Atlantic basins were limited. We interpret the late Coniacian–early Santonian depositional environment to be an oxygen minimum zone in a more open marine outer shelf or upper slope setting. A sudden increase in the proportion of deep-water agglutinated foraminifers in Sample 159-959D-65R-5, 30–34 cm, points to rapid deepening during the early Santonian. The higher diversity and the abundance of cosmopolitan taxa in samples from Cores 159-959D-66R and 159-959D-65R indicate that deep circulation between the North and South Atlantic was well established by the middle Coniacian to early Santonian.

INTRODUCTION

During drilling of Ocean Drilling Program Leg 159 on the Côte d'Ivoire-Ghana Transform Margin (CIGTM), a distinctive sequence of phosphatic hardgrounds—heavily bioturbated homogeneous silty clays with high amounts of terrigenous detritus, sandy limestones, and laminated and nonlaminated black claystones—was recovered in Cores 159-959D-66R through 68R. Of particular interest within Core 159-959D-68R are black fissile shales of the *W. archeoretacea* zone with a high total organic carbon (TOC), similar to sediments drilled from the Guinean slope during the *Equamarge II* cruise, which correspond to the global anoxic event of the Cenomanian/Turonian Boundary Event (CTBE) (Moullade et al., 1993). The Turonian to Santonian sediments from Hole 959D are partly characterized by high TOC, and contain some well-preserved benthic foraminifer assemblages, which are especially important for understanding the early paleoenvironments of the CIGTM and for retracing the paleoceanographic evolution of the Atlantic gateway during mid-Cretaceous times. The opening of this equatorial seaway between the North and South Atlantic was initiated in the Early Cretaceous, following the rifting between the African and South American continents (de Klasz, 1978; Moullade and Guérin, 1982; Moullade et al., 1993; Bonatti et al., 1996). During the early stages of continental breakup, the area was a key oceanic gateway, which first enabled the change from an equatorial oceanic circulation regime to the meridional circulation scenario characteristic of the present-day ocean. In their gen-

eral circulation model, Kruijs and Barron (1990) predicted strong upwelling systems in marginal basins of northwest Africa, with associated extended oxygen minimum zones for the mid-Cretaceous. Benthic foraminifer assemblages characteristic of high productivity upwelling conditions were recorded from Upper Cretaceous sediments of the Casamance Shelf off Senegal (Ly and Kuhnt, 1994; Kuhnt and Wiedmann, 1995) and from Cenomanian–Turonian sequences of the Tarfaya Coastal Basin off Morocco (Kuhnt and Wiedmann, 1995). In this study we document the taxonomic composition of benthic foraminifer assemblages at Site 959D, from the CTBE to the Santonian (Cores 159-959D-68R through 66R) and we discuss the response of benthic foraminifers to high organic carbon fluxes and to changing paleoceanographic conditions in the enlarging oceanic gateway.

LOCATION AND GEOLOGICAL SETTING

Hole 959D is situated on the northern flank of the Côte d'Ivoire-Ghana Marginal Ridge (CIGMR) at 3°37.656'N, 2°44.149'W in a water depth of 2090.7 m, on a small plateau close to the top of the CIGMR, as shown in Figure 1. The opening of the equatorial seaway between Africa and South America was initiated by crustal thinning and complex en echelon strike-slip faulting at the rifted basin and uplifted transform boundary in the Deep Ivorian Basin during the Early Cretaceous (Masle, Lohmann, Clift, et al., 1996). In the late Albian to early Cenomanian, northward prograding marine sequences were being deposited in developing halfgrabens and in distal fans along the steeper northern slopes of the CIGMR. As the Atlantic gateway continued to widen and to deepen during the Late Cretaceous, marine sedimentation proceeded on the northern flank of the CIGMR by aggradation of sediments derived from the African coast and by progradation of sediments eroded from the marginal ridge. Masle et al. (1997) suggested that maximum uplift of the marginal ridge occurred

¹Masle, J., Lohmann, G.P., and Moullade, M. (Eds.), 1998. *Proc. ODP, Sci. Results*, 159: College Station, TX (Ocean Drilling Program).

²Geologisch-Paläontologisches Institut der Christian-Albrechts-Universität zu Kiel, Olshausenstr. 40, D-24118 Kiel, Federal Republic of Germany.

³Present address: Department of Palaeontology, Natural History Museum, Cromwell Road, London SW7 5BD, United Kingdom. a.holbourn@nhm.ac.uk

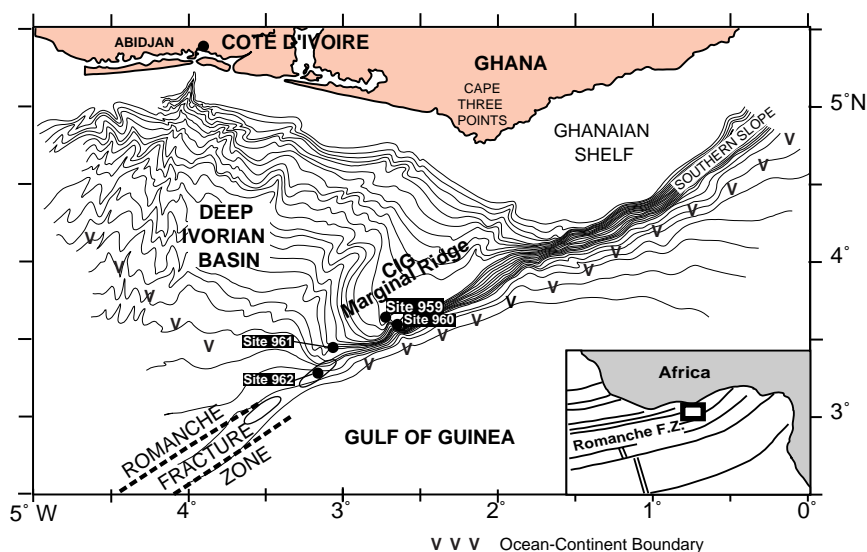


Figure 1. Location of Site 959.

between the Turonian and the Santonian and that the region underwent rapid subsidence after the late Santonian when black shales were being deposited at Hole 959D.

LITHOLOGY AND STRATIGRAPHY

The lower Turonian sediments (Core 159-959D-68R) from this site correspond to the lower part of lithologic Unit IVA, and consist of calcareous sandstone including thin conglomeratic beds with phosphatic pebbles and glauconitic clasts. Intercalated are black fissile shales with planktonic foraminifers of the *W. archaeocretacea* Zone that have high TOC values, and correspond to the global anoxic event of the CTBE. The upper Turonian to lower Coniacian sediments (Core 159-959D-67R), from the upper part of lithologic Unit IVA, are comprised of sandy limestone and sandy dolomite, which are heavily bioturbated at some levels. A phosphatic hardground in Section 159-959D-66R-CC marks the boundary between the lower Coniacian and the middle Coniacian (Watkins et al., Chap. 26, this volume). The middle Coniacian to lower Santonian sediments in Core 159-959D-66R above this hardground and at the base of Core 159-959D-65R are characterized by sequences of massive, black claystone alternating with finely laminated dark brown claystone, corresponding to the lowermost part of lithologic Unit 3. Phosphatic hardgrounds are present in Sections 159-959D-66R-4 through 66R-7 and a phosphatic conglomerate occurs in interval 66R-6, 111–118 cm, probably formed from the erosion of another hardground.

An early Turonian age was determined for Core 159-959D-68R and a late Turonian to early Coniacian age for Core 67R, based on nannofossil data (Watkins et al., Chap. 26, this volume). Four nannofossil subzones were recognized in Core 159-959D-66R by these authors: (1) an early Coniacian age was attributed to the base of Core 66R; (2) a middle Coniacian age to the interval between Sample 66R-7, 8–11 cm, and Sample 66R-6, 104–106 cm; (3) a late Coniacian age to the interval between Sample 66R-6, 47–50 cm and Sample 66R-5, 92–94 cm; and (4) a late Coniacian to early Santonian age to the upper part of Core 66R and the base of Core 65R. No planktonic foraminifers were recovered from Core 159-959D-67R, and the planktonic assemblage in Core 66R was dated as Coniacian to early Santonian by Bellier (Chap. 27, this volume).

METHODS

A total of 23 samples (~20 cm³) from four cores (Sections 159-959D-65R-5 through 68R-1) were analyzed. The samples were dried, weighed, soaked in distilled water, and wet-sieved through a 63-µm

(#230 mesh) screen; then, the residue was dried. Consolidated samples were first treated with a buffered 5% hydrogen peroxide solution to help the breakup before sieving. In rare cases where the hydrogen peroxide treatment did not lead to complete disintegration of the clay, the dried samples were soaked in a concentrated anionic tenside solution (REWOQUAT of REWO Chemie, Steinau an der Straße, Federal Republic of Germany), which usually disintegrated even slightly silicified samples. Generally, the complete residue was picked for benthic foraminifers. In a few exceptional cases with extremely high faunal content, samples were split with a standard Otto-splitter. Fragments of tubular species were counted as one individual; indeterminate fragments or extremely deformed specimens were picked but not included in the counts. Benthic foraminifer data are displayed in Table 1. The foraminifer slides are housed in the micropaleontology collections of the Geologisch-Paläontologisches Institut at the Christian Albrechts University in Kiel, where electron micrographs were also made on a Camscan SEM.

TOC values were performed on dried, homogenized samples at Bremen University, using a Leco CS-300 device. TOC data cited in the text and shown on Table 1 are from T. Wagner (pers. comm., 1996) and Pletsch et al. (in press).

The Shannon-Weaver information function (Shannon and Weaver, 1949) was used to evaluate benthic foraminifer diversity. This measure of heterogeneity is frequently used as an index of biodiversity. It takes into account the number of species and the equitability of their distribution within a sample. It is defined by the equation

$$H(S) = -\sum_{i=1}^s p_i \ln p_i$$

where S is the number of species and p_i the proportion of the i th species (p = percent divided by 100).

RESULTS

Biostratigraphy

Although many of the benthic foraminifers from Cores 159-959D-66R through 68R were long-ranging taxa in the Late Cretaceous, some species appear to have stratigraphical significance. Among the *Praeulimina* from Core 159-959D-68R, there is a particularly striking triserial form with markedly elongated spined chambers, referred to as *Praeulimina* sp. 1 in this work, which was previously illustrated as *Gabonita spinosa* by Petters (1982) from the lower Turonian of the South Benue Trough. *Bolivina anambra*, an

Table 1. Benthic foraminifer data for Sections 159-959D-65R-5 through 68R-1.

	65R-5, 30-34	65R-6, 28-32	65R-7, 31-35	66R-1, 21-25	66R-1, 68-71	66R-1, 110-114	66R-2, 19-22	66R-3, 20-23	66R-4, 21-23	66R-4, 68-70	66R-5, 18-21	66R-6, 15-17	66R-7, 21-25	67R-1, 4-8	67R-1, 68-71	67R-1, 140-144	67R-2, 26-30	67R-2, 77-81	67R-2, 118-122	68R-1, 20-24	68R-1, 40-44	68R-1, 82-84	68R-1, 85-88
Diverse Agglutinated	205																						
<i>Tristix</i> sp.				1																			
<i>Bathysiphon</i> sp.				6																			
? <i>Ammosphaeroidina</i> sp.				4	3																		
<i>Gaudryina pyramidata</i>							1																
<i>Vaginulinopsis</i> sp.							1																
<i>Citharina</i> sp.									2														
<i>Margulinopsis</i> sp.							2		1														
<i>Margulinopsis lituola</i>	2			1			1	1	3														
<i>Lenticulina macrodisca</i>	9						2	1	11														
<i>Ellipsoidina abbreviata</i>				11			9	5	7														
<i>Nodosarella</i> sp.				17				1	3														
<i>Lituotuba</i> sp.									1														
<i>Rhizammina</i> spp.			3	16			10		4														
<i>Oolina</i> spp.					1			1	1	1													
<i>Astacolus parallelus</i>	1			3			1	1	1	2													
<i>Laeidentalina catenula</i>	5			1	1			1	2	1													
<i>Ellipsoidella</i> sp.	1			1			1	2	6	3													
<i>Pyramidulina tetragona</i>				1						1													
<i>Nodosaria aspera</i>	1				1		2				1												
<i>Stilostomella alexanderi</i>				3	4			4		14	2												
<i>Lenticulina muensteri</i>				1	5		4	8		5	1												
<i>Psilocitharella recta</i>							1				1												
<i>Lingulina taylorana</i>							1				1												
<i>Pyrulina cylindroides</i>				7	4		2		4	1	3												
<i>Ramulina globotubulosa</i>					1						3												
<i>Ramulina aculeata</i>				25	5		4			7	27												
<i>Bandyella greatvalleyensis</i>	1			1	3		3	1	9		2												
<i>Gyroidinoides subangulatus</i>	14	2	4	18	10	1	21	2	42	22	43												
<i>Astocolus</i> spp.	4			1			1		6	2	2												
<i>Saracenaria triangularis</i>				1		3	1	1		2													
<i>Pleurostomella</i> spp.	5	1		10	8		1	8		20	27												
<i>Neobulimina subregularis</i>		18	24		36	71	63	9		9	247												
<i>Buliminella cf. gabonica</i>	4	6	6	10	17	8	36		4	12	97												
<i>Siphogenerinoides pygmaea</i>			1		5			1		1													
<i>Laeidentalina soluta</i>											2												
<i>Pyramidulina</i> sp.				2				1			3												
<i>Stilostomella</i> spp.	5	1		15	6	1	3		18	12	12												
<i>Hemibulimina bullata</i>								1			2												
<i>Cibicides dayi</i>							16					1											
<i>Conorotalites michelianus</i>				70	8		34	10	7	55	30	1											
<i>Praebulimina fang</i>				9	10		17	14	7	42	131	2											
<i>Planulina complanata</i>	14			12	6		10		5	18	11		2										
<i>Praebulimina robusta</i>	22		5	59	22		26	6		34	183	2	2										
<i>Praebulimina proluxa longa</i>				3			3	1		2	13	1	40										
<i>Gyroidinoides</i> spp.								1		4	27												
<i>Gyroidinoides ex gr. nitidus</i>	2			8																			
<i>Nothia ex gr. excelsa</i>																							
<i>Reophax</i> sp.							2																
<i>Rhabdammina</i> spp.																							
<i>Dorothia filiformis</i>				8					3														
<i>Bulbobaculites</i> sp.				4			3		2					45									
<i>Recurvoides</i> sp.				5																			
? <i>Silicosignolina</i> sp.																							
<i>Lenticulina</i> spp.	19		3	3	1	1	2	1	8		2			15						6	1		
<i>Neoflabellina</i> sp.																							1
<i>Lenticulina rotulata</i>	14			2	1				1	1											1	1	
<i>Ramulina</i> spp.	12		1	6			4		2		3										1	1	1
<i>Bolivina anambra</i>															21						40	45	57
<i>Praebulimina</i> sp. 3																					36	18	13
<i>Praebulimina</i> sp. 2																					24	114	14
<i>Praebulimina</i> sp. 1																					2	89	1
<i>Laeidentalina</i> spp.	78		1	52	4		22		21	30	74		1								2	4	2
<i>Conorotalites</i> sp.	4																						1
<i>Gavelinella</i> sp. 1																							1
<i>Gavelinella</i> spp.		31	11	2	3	24	3	3		3	62	1	127		11						14	13	75
<i>Citharinella</i> sp.																							217
<i>Praebulimina</i> spp.																						1	4
<i>Bolivina</i> spp.	3	8				6	1	3		5	3				2						5		2
<i>Bolivina</i> sp.					1		2			3	7		37										1
Number of specimens:	425	67	59	398	167	112	317	86	185	304	1040	11	229	62	34	17	0	2	10	125	323	171	279
Shannon-Weaver index:		1.4	1.8	2.9	2.7	1.1	2.8	2.8	2.8	2.6	2.5	1.9	1.3	0.7	0.8	1.0	0	0.7	1.2	1.6	1.6	1.4	1.4
TOC:	2.4	11.2	14.1	4.0	4.0*	10.8	2.3	3.2	3.9	4.1	3.1	16.6	6.2	1.1	1.0	1.1	0.5	0.5	1.0	2.7	2.9	3.9	2.0
Age:	early Santonian to early Coniacian													late Turonian				early Turonian					

Note: TOC = total organic carbon. * = value for close sample.

other characteristic taxon in the assemblage from Core 159-959D-68R, was also originally described by Petters (1982) from the lower Turonian of Nigeria. The early Turonian age of Core 159-959D-68R is constrained by the occurrence of large-sized planktonic foraminifers of the genus *Whiteinella* (*W. aprica* and *W. archaeocretacea*). The buliminids from Core 159-959D-66R consist mainly of species, initially described by de Klasz and Rérat (1962) and de Klasz et al. (1963) from western equatorial African basins. *Praebulimina fang* and *Praebulimina robusta* are long-ranging Late Cretaceous species, known to occur from the early Turonian to the Maastrichtian in Gabon, Cameroon, and Nigeria (de Klasz et al., 1963). *Praebulimina proluxa longa* and *Neobulimina subregularis* were recorded in the "Senonian" of Gabon by de Klasz et al. (1963). The stratigraphic distribution of selected Cretaceous buliminids and bolivinids in equatorial basins is shown in Figure 2.

Faunal Distribution

Three distinct benthic foraminifer assemblages are recognized from Core 159-959D-68R to the base of Core 65R (Section 65R-5), which exhibit considerable differences in composition (Table 1):

1. *Praebulimina* sp. 1 - *Praebulimina* sp. 2 - *Bolivina anambra* Assemblage, Core 159-959D-68R, Age: early Turonian

This relatively low-diversity assemblage (Shannon-Weaver index between 0.97 and 1.63) is numerically dominated by *Bolivina anambra*, *Praebulimina* sp. 1, *Praebulimina* sp. 2, *Praebulimina* sp. 3, and *Gavelinella* spp. The number of *Gavelinella* spp. in the samples is highly variable, being highest at the base of the interval.

2. *Bulbobaculites* sp. - *Recurvoides* sp. Assemblage, Core 159-959D-67R, Age: late Turonian to early Coniacian

This low-abundance and low-diversity assemblage (Shannon-Weaver index between 0.69 and 1.23) contains organically cemented agglutinated taxa including *Bulbobaculites* sp. and *Recurvoides* sp. and/or some corroded tests of *Lenticulina*, *Bolivina Gyroidinoides* ex gr. *nitidus*. A few samples are virtually barren.

3. *Praebulimina robusta* - *Neobulimina subregularis* - *Gyroidinoides subangulatus* Assemblage, Core 159-959D-66R and Sections 159-959D-65R-7 through 65R-5, Age: middle Coniacian to early Santonian

This assemblage is generally abundant and diverse (Shannon-Weaver index 2.5 or above), but displays marked drops in abundance and diversity in Samples 159-959D-66R-7, 21–25 cm; 66R-6, 15–17 cm; 66R-1, 110–114 cm; 65R-7, 31–35 cm; and 65R-6, 28–32 cm (Shannon-Weaver index between 1.09 and 1.85). These fluctuations appear related to changes in TOC values (Table 1). Diversity and abundance are extremely low in Sample 159-959D-66R-6, 15–17 cm, where TOC reaches over 16%. Diversity is low and abundance relatively high in Sample 159-959D-66R-7, 21–25 cm, which is strongly dominated by gavelinellids and buliminids and where TOC exceeds 6%. Except for Sample 159-959D-66R-1, 110–114 cm, all samples in the upper part of Core 159-959D-66R have lower TOC values (between 2% and 4%) and display higher diversity and abundance. Common genera are *Praebulimina*, *Buliminella*, *Neobulimina*, *Conorotalites*, *Gyroidinoides*, *Gavelinella*, *Pleurostomella*, *Nodosarella*, *Stilostomella*, *Lenticulina*, *Laevidentalina*, *Astacolus*, *Planularia*, *Marginulinopsis*, *Pyramidulina*, and *Saracenaria*. The composition of the buliminid associations differs markedly from that in Core 159-959D-68R and comprises *Praebulimina robusta*, *Praebulimina proluxa longa*, *Praebulimina fang*, *Neobulimina subregularis* and *Buliminella* cf. *gabonica*. Diversity and abundance are low in Samples 159-959D-65R-7, 31–35 cm, and 65R-6, 28–32 cm,

Age	Turonian	Coniacian	Santonian	Campanian	Maastrichtian
<i>Buliminella quadrilobata</i>		—	—	—	—
<i>Neobulimina subregularis</i>		—	—	—	—
<i>Praebulimina bantu</i>		—	—	—	—
<i>Praebulimina crassa</i>				—	—
<i>Praebulimina fang</i>		—	—	—	—
<i>Praebulimina robusta</i>		—	—	—	—
<i>Praebulimina proluxa</i>		—	—	—	—
<i>Praebulimina arkadelphiana</i>					—
<i>Praebulimina</i> sp. 1	—				
<i>Bolivina anambra</i>	—				
<p> </p>					

Figure 2. Distribution of stratigraphically important Cretaceous buliminids and bolivinids in equatorial Atlantic basins, compiled from Tronchetti (1981), Petters (1982), Koutsoukos (1992), Ly and Kuhnt (1994), A. Holbourn and W. Kuhnt (unpubl. data), and this work.

where TOC values are above 11%. A marked change in faunal composition occurs in Sample 65R-5, 30–34 cm, with a TOC value of 2.35%, where numerous nodosariids and agglutinated tests are recorded together with a few buliminids.

DISCUSSION

Faunal Changes and TOC

Fluctuations in the abundance and diversity of foraminifer assemblages in Cores 159-959D-68R and 66R appear related to changes in TOC values (Fig. 3), and regression analysis indicates a negative correlation between TOC and the Shannon-Weaver index for Core 159-959D-66R (Fig. 4). A low-diversity foraminifer assemblage dominated by buliminids, bolivinids, and gavelinellids is found in samples from the black homogeneous claystone in Core 159-959D-68R with consistently high TOC values (2.5% to 3.9%). Marked variations are evident in Core 159-959D-66R, where the lowest Shannon-Weaver index values are recorded in samples from dark, finely laminated claystone, where buliminids show strong dominance and TOC is extremely high (between 11% and 17%). The very high TOC values and the absence of bioturbation in these laminated intervals indicate that the sediment was probably almost anoxic and close to abiotic at the time of deposition. Higher diversity is found in samples from the massive, homogeneous claystone, where TOC fluctuates between 2% and 4%. Oxygen depletion must have been less severe during the deposition of these non-laminated intervals, and more diversified benthic communities were able to become established. A typical example of this sedimentary and faunal cyclicity, which is recurrent throughout Core 159-959D-66R, is shown in Figure 3.

Paleoenvironment

Assemblage 1

The low diversity and strong dominance of buliminids and bolivinids in the assemblage together with the relatively high TOC values suggest poorly oxygenated bottom waters in an outer shelf or upper slope setting. Low-diversity benthic foraminifer assemblages dominated by a few species of *Bolivina* and *Bulimina* in unusually high numbers were previously described from recent oxygen-depleted environments by Phleger and Soutar (1973), Basov (1979), Sen Gupta et al. (1981). Recent benthic foraminifer assemblages within the upper part of an intense oxygen minimum zone on the outer shelf of the northwest Arabian Sea were also found to be dominated by *Bolivina pygmaea* and *Bulimina* sp. 1 (Hermelin and Shimmield, 1990; Hermelin, 1992). Similar assemblages were documented by de Klasz et al. (1963) from the Turonian of Gabon and by Koutsoukos and Hart (1990) and Koutsoukos et al. (1990) from the lower Turonian of the Sergipe Basin of Brazil. Koutsoukos (1992) suggested that rising sea levels, sluggish circulation, and salinity stratification in deep oceanic basins, together with periodic high runoff and/or local upwelling, were responsible for widespread dysoxic conditions in the Sergipe Basin in the early Turonian. The Deep Ivorian Basin probably also had a restricted physiography favoring stagnation in the early Turonian, as the prominent ridge of the transform margin must have acted as a barrier between the marginal basin and the widening Equatorial Atlantic.

Assemblage 2

TOC values drop significantly in Core 159-959D-67R (remaining ~1% or less), which consists of bioturbated sandy limestone and sandy dolomite. Abundance and diversity of the benthic foraminifer assemblage are extremely low in the samples examined from this core. The high corrosion of the calcareous tests present in some sam-

ples suggests that they are allochthonous. This interval may represent a regressive episode in the late Turonian–early Coniacian, during which terrigenous sedimentation increased in a more proximal setting and the oxygen minimum zone shifted further out into the basin.

Assemblage 3

The assemblage composition and high TOC values suggest that oxygen minima were established on the outer shelf or upper slope of the basin from the middle Coniacian to the early Santonian. Intermittent increases in benthic foraminifer diversity in Core 159-959D-66R and at the base of Core 65R and corresponding decreases in TOC probably reflect episodic improvements in bottom-water oxygenation as periodic contraction or expansion of the oxygen minimum zone led to changes in its depth range and intensity.

An increase in paleodepth is indicated in Section 159-959D-66R-1 with the appearance of a few deep-water agglutinated foraminifers (DWAF) at the top of the section. A considerable increase in the proportion of DWAF is observed in Sample 159-959D-65R-5, 30–34 cm, where they represent approximately 50% of the assemblage. Above this sample the remaining Upper Cretaceous sequence contains mainly DWAF with organic cement, which are diagnostic of deposition close to the carbonate compensation depth (CCD) (Kuhnt et al., Chap. 31, this volume). The sudden increase in the proportion of DWAF in the early Santonian (Sample 159-959D-65R-5, 30–34 cm) and the disappearance of all calcareous taxa in Core 159-959D-64R suggest rapid deepening below a local CCD in the late Santonian.

Previous sedimentological and micropaleontological studies (Wiedmann et al., 1982; Thurow et al., 1982; Kuhnt et al., 1986; Ly and Kuhnt, 1994) and the general circulation model of Kruijs and Barron (1990) proposed that the whole of the northwest African Margin was exposed to intense coastal upwelling during the Late Cretaceous, leading to the expansion and intensification of the oxygen minimum zone. The organic-rich sediments in Cores 159-959D-66R, associated with phosphatic crusts and hardground, may, thus, be interpreted as indicators of high productivity (Parrish et al., 1993; Parrish, 1995) because favorable conditions for their formation were created during high organic matter fluxes (Mullins et al., 1985; Parrish, 1995). Alternatively, the cyclic depletion of oxygen at the seafloor may have resulted from restricted circulation in a shallow, semi-enclosed basin, where periodic sea-level fluctuations, perhaps linked to subsidence, induced intermittent reoxygenation of stagnant bottom waters. According to this interpretation, the phosphatic hardgrounds in Core 159-959D-66R would have formed during periods of slow sedimentation and represent hiatuses in sedimentation during highstands of sea level.

Paleobiogeography

The two buliminid associations found in Cores 159-959D-68R and 66R have distinct composition, although many of the taxa appear to have extended stratigraphic ranges. The early Turonian association in Core 159-959D-68R, characterized by *Praebulimina* sp. 1, *Praebulimina* sp. 2, *Praebulimina* sp. 3, and *Bolivina anambra*, represents a typical “African” assemblage, previously only recorded in the Nigerian Benue Trough, and lacks the typical *Gabonita* biofacies widely recorded in the Tarfaya, Casamance, and Sergipe Basins and in Gabon (Koutsoukos, 1992; Kuhnt and Wiedmann, 1995). By contrast, the middle Coniacian to early Santonian association in Core 159-959D-66R with *Praebulimina robusta*, *Praebulimina proluxa longa*, *Praebulimina fang*, *Neobulimina subregularis*, and *Buliminea cf. gabonica*, had wider distribution on tropical shelves and upper slopes of the Gulf Coast, Caribbean and Guinean Provinces (Koutsoukos, 1992) and Casamance Shelf (Ly and Kuhnt, 1994). This sug-

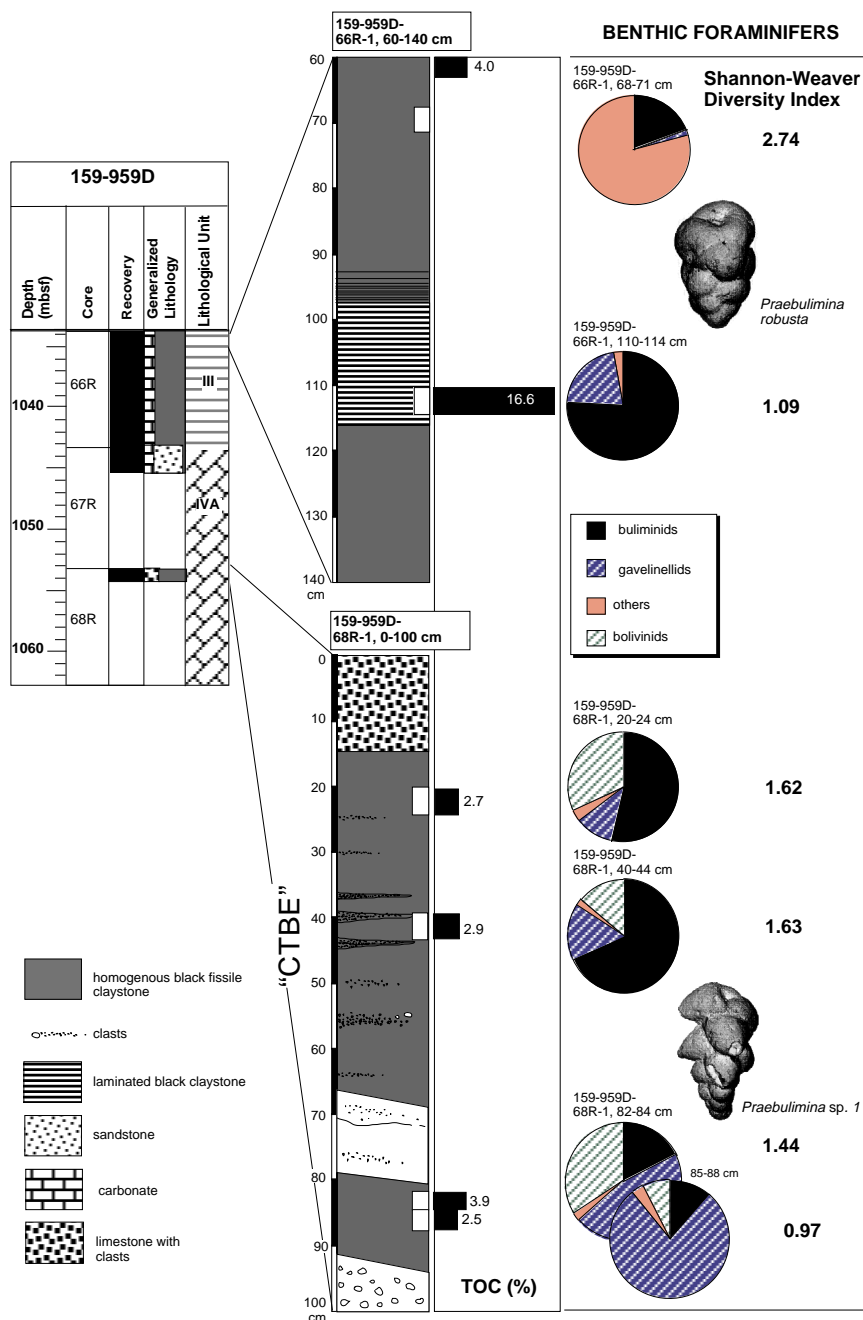


Figure 3. Benthic foraminifer distribution in Hole 959D in relation to TOC and lithology (representative species are shown for the distinct buliminid associations present in Cores 159-959D-68R and 66R).

gests that endemism was stronger in western African basins during the early Turonian when circulation patterns were more restricted. The wider biogeographic distribution during the middle Coniacian to early Santonian provides evidence for more open connections between equatorial Atlantic basins and for comparable paleoenvironmental conditions at low latitudes. The occurrence of cosmopolitan taxa in the more diversified samples from Core 159-959D-66R and the abundance of DWAF in Sample 159-959D-65R-5, 30–34 cm, also demonstrate that deep circulation was well established between the North and South Atlantic by the middle Coniacian to early Santonian.

CONCLUSION

Turonian to Santonian benthic foraminifer assemblages from the western African equatorial margin establish paleobathymetric con-

straints for the deposition of the Turonian to Santonian sedimentary sequences at Hole 959D. Upper bathyal paleodepths must have prevailed from the early Turonian to early Santonian at Hole 959D for the area to have remained within depths of the expanded oxygen minimum zone. During the early Santonian, a sudden increase in the proportion of DWAF in Sample 159-959D-65R-5, 30–34 cm, points to a rapid deepening.

The benthic foraminifer data provide evidence that an intensified oxygen minimum zone became established off the Côte d'Ivoire-Ghana Transform Margin in the early Turonian and in the middle Coniacian to early Santonian. Intermittent increases in benthic foraminifer diversity in Core 159-959D-66R and at the base of Core 159-959D-65R and corresponding decreases in TOC probably reflect episodic improvements in bottom-water oxygenation as periodic contraction/expansion of the oxygen minimum zone led to changes in its depth range and intensity.

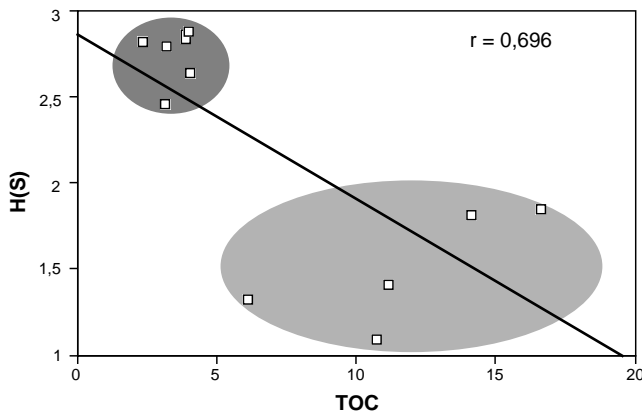


Figure 4. Regression analysis between TOC and Shannon-Weaver index for Core 159-959D-66R.

The distinct composition of the two buliminid associations found in Cores 159-959D-68R and 66R suggests that endemism was stronger during the early Turonian when circulation was probably more restricted in the Deep Ivorian and Benue Basins. By contrast, the widespread distribution of the buliminid association in low latitudes during the middle Coniacian to early Santonian indicates more open connections between the Deep Ivorian Basin and other equatorial Atlantic basins. The occurrence of cosmopolitan taxa in the more diversified samples from Core 159-959D-66R and the abundance of DWAF in Sample 159-959D-65R-5, 30–34 cm, demonstrate that deep circulation was well established between the North and South Atlantic in the middle Coniacian to early Santonian.

ACKNOWLEDGMENTS

We are especially grateful to Malcolm Hart and Claudia Schröder-Adams for reviewing the manuscript, to Thomas Pletsch for very helpful comments and discussions, and to Thomas Wagner for supplying TOC data. We extend our thanks to the staff of the SEM Lab and Photographic Unit at the Geologisch-Paläontologisches Institut of the Christian Albrechts University in Kiel. AELH acknowledges support of a Royal Society European Exchange Fellowship at Kiel University. This project was funded by a DFG grant (Ku 649/2) to WK.

REFERENCES

- Bartenstein, H., 1954. Revision von Berthelin's Mémoire 1880 über die Alb-Foraminiferen von Montcley. *Senckenbergiana Lothaea*, 35 (1/2): 35–50.
- Bartenstein, H., and Bolli, H.M., 1986. The Foraminifera in the Lower Cretaceous of Trinidad, W.I. Part 5: Maridale Formation, upper part; *Hedbergella rohri* zone. *Eclogae Geol. Helv.*, 7:945–999.
- Basov, I.A., 1979. Ecology of benthic foraminifera in the upwelling zone near south-west Africa. *Voprosy Mikropaleontol., Moscow*, 22:135–146. (in Russian)
- Basov, I.A., and Krashennikov, V.A., 1983. Benthic foraminifera in Mesozoic and Cenozoic sediments of the southwestern Atlantic as an indicator of paleoenvironment, Deep Sea Drilling Project Leg 71. In Ludwig, W.J., Krashennikov, V.A., et al., *Init. Repts. DSDP*, 71: Washington (U.S. Govt. Printing Office), 739–788.
- Bolli, H.M., Beckmann, J.-P., and Saunders, J.B., 1994. *Benthic Foraminiferal Biostratigraphy of the South Caribbean Region*: Cambridge (Cambridge Univ. Press).
- Bonatti, E., Ligi, M., Borsetti, A.M., Gasperini, L., Negri, A., and Sartori, R., 1996. Lower Cretaceous deposits trapped near the equatorial Mid-Atlantic Ridge. *Nature*, 380:518–520.
- Cushman, J.A., 1926. The foraminifera of the Velasco Shale of the Tampico Embayment. *Am. Assoc. Pet. Geol., Bull.* 10 (1/6): 581–612.
- , 1936. New genera and species of the families Vemeuilinidae and Valvulinidae and of the subfamily Virguliniinae. *Spec. Publ. Cushman Lab. Foraminiferal Res.*, 6:1–89.
- , 1938. Additional new species of American Cretaceous foraminifera. *Contrib. Cushman Lab. Foraminiferal Res.*, 14:31–52.
- Dam, A., 1950. Les Foraminifères de l'Albien des Pays-Bas. *Mem. Soc. Geol. Fr.*, 63:1–67.
- de Klasz, I., 1978. The West African sediments. In Moullade, M., and Nairn, A.E.M. (Eds.), *The Phanerozoic Geology of the World. II. The Mesozoic*, A:371–399.
- de Klasz, I., Magné, J., and Rérat, D., 1963. Quelques formes nouvelles de Buliminidae caractéristiques du Crétacé supérieur du Gabon (Afrique Équatoriale). *Rev. Micropaleontol.*, 6:145–152.
- de Klasz, I., and Rérat, D., 1962. Quelques nouveaux foraminifères du Crétacé et du Tertiaire du Gabon (Afrique Équatoriale). *Rev. Micropaleontol.*, 4:175–189.
- d'Orbigny, A., 1840. Mémoire sur les Foraminifères de la craie blanche du Bassin de Paris. *Mem. Soc. Geol. Fr.*, 4:1–51.
- Geroch, S., and Nowak, W., 1984. Proposal of zonation for the late Tithonian-Eocene, based upon the arenaceous foraminifera from the outer Carpathians, Poland. In Oertli, H.J. (Ed.), *BENTHOS '83: 2nd Int. Symp. Benthic Foraminifera*. Bull. Cent. Rech. Explor.-Prod. Elf-Aquitaine, 6:225–239.
- Guerin, S., 1981. Utilisation des foraminifères planctiques et benthiques dans l'étude des paleo-environnements océaniques au Crétacé moyen: application au matériel des forages D.S.D.P. de l'Atlantique nord et sud. Comparaison avec la Téthys [Thèse Doctorat]. Univ. Nice.
- Hermelin, J.O.R., 1992. Variations in the benthic foraminiferal fauna of the Arabian Sea: a response to changes in upwelling intensity? In Summerhayes, C.P., Prell, W.L., and Emeis, K.C. (Eds.), *Upwelling Systems: Evolution Since the Early Miocene*. Geol. Soc. Spec. Publ. London, 64:151–166.
- Hermelin, J.O.R., and Shimmield, G.B., 1990. The importance of the oxygen minimum zone and sediment geochemistry on the distribution of Recent benthic foraminifera from the NW Indian Ocean. *Mar. Geol.*, 91:1–29.
- Kaiho, K., Fujiwara, O., and Motoyama, I., 1993. Mid-Cretaceous faunal turnover of intermediate-water benthic foraminifera in the northwestern Pacific Ocean margin. *Mar. Micropaleontol.*, 223:13–49.
- Kaminski, M.A., and Geroch, S., 1993. A revision of foraminiferal species in the Grzybowski Collection. In Kaminski, M.A., Geroch, S., and Kaminski, D.G. (Eds.), *The Origins of Applied Micropaleontology: The School of Józef Grzybowski*. Grzybowski Found. Spec. Publ., 1:239–323.
- Koutsoukos, E.A.M., 1992. Late Aptian to Maastrichtian foraminiferal biogeography and paleoceanography of the Sergipe Basin, Brazil. *Palaeogeogr., Palaeoclimatol., Palaeoecol.*, 92:295–324.
- Koutsoukos, E.A.M., and Hart, M.B., 1990. Cretaceous foraminiferal morphogroup distribution patterns, paleocommunities and trophic structures: a case study from the Sergipe Basin, Brazil. *Trans. R. Soc. Edinburgh: Earth Sci.*, 81:221–246.
- Koutsoukos, E.A.M., Leary, P.N., and Hart, M.B., 1990. Latest Cenomanian-earliest Turonian low-oxygen tolerant benthic foraminifera: a case study from the Sergipe Basin (N.E. Brazil) and the western Anglo-Paris basin (southern England). *Palaeogeogr., Palaeoclimatol., Palaeoecol.*, 77:145–177.
- Kruijs, E., and Barron, E., 1990. Climate model prediction of paleoproductivity and potential source rock distribution. In Huc, A.Y. (Ed.), *Deposition of Organic Facies*. AAPG Stud. in Geology, 30:195–216.
- Kuhnt, W., Thurow, J., and Herbin, J.P., 1986. Oceanic anoxic conditions around the Cenomanian/Turonian Boundary and the response of the biota. In Degens, E.T., Meyers, P.A., and Brassell, S.C. (Eds.), *Biogeochemistry of Black Shales*. Mitt. Geol. Inst. Hamburg, 60:205–246.
- Kuhnt, W., and Wiedmann, J., 1995. Cenomanian-Turonian source rocks: paleobiogeographic and paleoenvironmental aspects. In Huc, A.Y. (Ed.), *Paleogeography, Paleoclimate and Source Rocks*. AAPG Stud. in Geol., 40:213–232.
- Lamarck, J.B., 1804. Suite des mémoires sur les fossiles des environs de Paris. *Ann. Mus. Nat. Hist. Nat.*, 5:179–357.
- Loeblich, A.R., Jr., and Tappan, H., 1988. *Foraminiferal Genera and Their Classification*: New York (Van Nostrand Reinhold).
- Ly, A., and Kuhnt, W., 1994. Late Cretaceous benthic foraminiferal assemblages of the Casamance shelf (Senegal, NW Africa): indication of a Late Cretaceous oxygen minimum zone. *Rev. Micropaleontol.*, 27:49–74.
- Magniez-Jannin, F., 1975. *Les Foraminifères de l'Albien de l'Aube: Paléontologie, Stratigraphie, Écologie*: Paris (Cahiers de Paléontologie).

- Masclé, J., Lohmann, P., and Clift, P., 1997. Development of a passive transform margin: Côte d'Ivoire-Ghana transform margin. ODP Leg 159 preliminary results. *Geo-Mar. Lett.*, 17:4–11.
- Masclé, J., Lohmann, G.P., Clift, P.D., et al., 1996. *Proc. ODP, Init. Repts.*, 159: College Station, TX (Ocean Drilling Program).
- McNeil, D.H., and Caldwell, W.G.E., 1981. Cretaceous rocks and their foraminifera in the Manitoba Escarpment. *Spec. Pap. Geol. Assoc. Can.*, 21:1–439.
- Meyn, H., and Vespermann, J., 1994. Taxonomische Revision von Foraminiferen der Unterkreide SE-Niedersachsens nach ROEMER (1839, 1841, 1842), KOCH (1851) und REUSS (1863). *Senckenbergiana Lethaea*, 74:49–272.
- Moullade, M., 1984. Intérêt des petits foraminifères benthiques "profonds," pour la biostratigraphie et l'analyse des paléoenvironnements océaniques Mésozoïques. In Oertli, H.J. (Ed.), *BENTHOS '83: Proc. 2nd Int. Symp. Benthic Foraminifera*. Bull. Cent. Rech. Expl.-Prod. Elf-Aquitaine, 6:429–464.
- Moullade, M., and Guérin, S., 1982. Le problème des relations de l'Atlantique Sud et de l'Atlantique Central au Crétacé moyen: nouvelles données microfauniques d'après les forages D.S.D.P. *Bull. Soc. Geol. Fr.*, 24:511–517.
- Moullade, M., Masclé, J., Benkhelil, J., Cousin, M., and Tricart, P., 1993. Occurrence of marine mid-Cretaceous sediments along the Guinean slope (Equamarge II cruise): their significance for the evolution of the central Atlantic African margin. *Mar. Geol.*, 110:63–72.
- Mullins, H.T., Thompson, J.B., McDougall, K., and Vercoutere, T.L., 1985. Oxygen-minimum zone edge effects: evidence from the Central California coastal upwelling system. *Geology*, 13:491–494.
- Neagu, T., 1975. Monographie de la faune des Foraminifères éocétacés du couloir de Dimboviciora, de Codlea et des Monts (Persani), (Couches de Carhaga). *Mem. Inst. Geol. Geophys.*, 25:1–141.
- Parrish, J.T., 1995. Paleogeography of C_{org}-rich rocks and the preservation versus production controversy. In Huc, A.Y. (Ed.), *Paleogeography, Paleoclimate and Source Rocks*. AAPG Stud. in Geol., 40:1–20.
- Parrish, J.T., Ziegler, A.M., and Humphreys, R.G., 1993. Upwelling in the Paleozoic Era. In Thiede, J., and Suess, E. (Eds.), *Coastal Upwelling: Its Sediment Record* (Pt. B): New York (Plenum Press): 553–578.
- Petters, S.W., 1982. Central West African Cretaceous-Tertiary benthic foraminifera and stratigraphy. *Palaeontographica A*, 179:1–104.
- Petters, S.W., and Ekweozor, C.M., 1982. Petroleum geology of the Benue Trough and southeastern Chad Basin, Nigeria. *Palaeogeogr., Palaeoclimatol., Palaeoecol.*, 40:311–314.
- Phleger, F.B., and Soutar, A., 1973. Production of benthic foraminifera in three east Pacific oxygen minima. *Micropaleontol.*, 19:110–115.
- Pletsch, T., Wagner, T., Holbourn A.E.L., Kuhnt, W., Erbacher, J., Söding, E., and Moullade, M., in press. Sedimentary dynamics along an opening oceanic gateway: the Cretaceous Côte d'Ivoire-Ghana Transform Margin (eastern Equatorial Atlantic, ODP Leg 159). *Geol. Soc. Spec. Publ.*
- Plummer, H.J., 1927. Foraminifera of the Midway formation in Texas. *Texas Univ. Bull.*, 2644.
- Reicherter, K., Pletsch, T., Kuhnt, W., Manthey, J., Homeier, G., Wiedmann, J., and Thurow, J., 1994. Mid-Cretaceous paleogeography and paleoceanography of the Betic Seaway (Betic Cordillera, Spain). *Palaeogeogr., Palaeoclimatol., Palaeoecol.*, 107:1–33.
- Reuss, A.E., 1844. *Geognostische Skizzen aus Böhmen* (Vol. 2): Prague.
- , 1845. *Die Versteinerungen der Böhmisches Kreideformation* (Vol. 1): Stuttgart (E. Schweizerbart).
- , 1846. *Die Versteinerungen der Böhmisches Kreideformation* (Vol. 2): Stuttgart (E. Schweizerbart).
- , 1851. Die Foraminiferen und Entomostraceen des Kreidemergels von Lemberg. *Naturwiss. Abh. Wein.*, 4:17–52.
- , 1860. Die Foraminiferen der Westphälischen Kreideformation. *Sitzungsber. Kais. Akad. Wiss. Wien Math.-Naturwiss. Kl.*, 40:147–238.
- , 1863. Die Foraminiferen des norddeutschen Hils und Gault. *Sitzungsber. Kais. Akad. Wiss. Wien Math.-Naturwiss. Kl.*, 46:5–100.
- Riegraf, W., and Luterbacher, H., 1989. Benthonische Foraminiferen aus der Unterkreide des "Deep Sea Drilling Project" (Leg 1–79). *Geol. Rundsch.*, 78:1063–1120.
- Roemer, F., 1839. *Die Versteinerungen des norddeutschen Oolithen-Gebirges*: Hannover.
- Roemer, F.A., 1838. Die Cephalopoden des norddeutschen tertiären Meeressandes. *Neues Jahrb. Miner., Geogr. Geol. Petref.*, 381–394.
- Scheibnerová, V., 1976. Cretaceous Foraminifera of the Great Australian Basin. *New South Wales Geol. Surv. Mem. Palaeontol.*, 17:1–265.
- Seguenza, G., 1859. Intorno ad un nuovo genere di foraminiferi fossili del torreno Miocenico di Messina. *Eco Peloritano*, 25:1–5.
- Sen Gupta, B.K., Lee, R.F., and May, M.S., 1981. Upwelling and an unusual assemblage of benthic foraminifera on the northern Florida continental slope. *J. Paleontol.*, 55:853–857.
- Shannon, C.E., and Weaver, W., 1949. *The Mathematical Theory of Communication*: Urbana (Univ. of Illinois Press).
- Thurow, J., Kuhnt, W., and Wiedmann, J., 1982. Zeitlicher und paläogeographischer Rahmen der Phthanit- und Black Shale-Sedimentation in Marokko. *Neues Jahrb. Geol. Palaeontol.*, 165:147–176.
- Tronchetti, G., 1981. Les foraminifères Crétacés de Provence (Aptien-Santonien) [Thèse Doctorat d'Etat]. Trav. Lab. Geol. Hist. Palaeontol., Univ. de Provence.
- Tronchetti, G., and Grosheny, D., 1991. Les assemblages de foraminifères benthiques au passage Cénomanien-Turonien à Vergons, S-E France. *Geobios*, 24:13–31.
- Trujillo, E.F., 1960. Upper Cretaceous foraminifera from near Redding, Shasta County, California. *J. Paleontol.*, 34:290–346.
- Weidich, K.F., 1990. Die kalkalpine Unterkreide und ihre Foraminiferenfauna. *Zitteliana*, 17, Abhandl. Bayerisch. Staatssam. Palaeontol. Hist. Geol.
- White, M.P., 1928. Some index foraminifera of the Tampico Embayment of Mexico (Part 2). *J. Paleontol.*, 2:177–215.
- Wiedmann, J., Butt, A., and Einsele, G., 1982. Cretaceous stratigraphy, environment and subsidence history at the Moroccan continental margin. In von Rad, U., Hinz, K., Sarntheim, M., and Seibold, E. (Eds.), *Geology of the Northwest African Continental Margin*: Berlin (Springer-Verlag), 366–395.

Date of initial receipt: 23 September 1996

Date of acceptance: 4 June 1997

Ms 159SR-038

TAXONOMIC NOTES

Original type references and references to subsequent well-illustrated citations are provided. Poorly preserved specimens, which could not be determined at the specific level, were left in open nomenclature (sp. or spp.). Well-preserved taxa that did not closely match any described species in the literature were given specific numbers (sp. 1, sp. 2, etc.).

Astacolus parallelus (Reuss, 1863)
Plate 1, Figure 4

Cristellarina parallela Reuss, 1863, pl. 7, figs. 1–2.
Astacolus parallelus (Reuss). Meyn & Vesperman, 1994, pl. 42, figs. 16–20; pl. 43, figs. 1–2.

Bandyella greatvalleyensis (Trujillo, 1960)
Plate 2, Figure 4

Pleurostomella greatvalleyensis Trujillo, 1960, pl. 50, figs. 5–6.
Bandyella greatvalleyensis (Trujillo), Loeblich & Tappan, 1988, pl. 584, figs. 21–22. Bolli et al., 1994, fig. 38. 17–18.

Bolivina anambra Petters, 1982
Plate 3, Figures 10, 11

Bolivina anambra Petters, 1982, pl. 11, figs. 21–22, 29.

Buliminella sp. cf. *gabonica altispira* de Klasz, Magné, & Rérat, 1963
Plate 2, Figure 13

Buliminella gabonica altispira de Klasz, Magné, & Rérat, 1963, pl. 1, fig. 3.

Cibicoides dayi (White, 1928)

Planulina dayi White, 1928, pl. 41, fig. 3.
Cibicoides dayi (White). Ly & Kuhnt, 1994, pl. 5, fig. 1.

Conorotalites michelinianus (d'Orbigny, 1840)
Plate 2, Figure 9

Rotalina micheliniana d'Orbigny, 1840, pl. 3, figs. 1–3.
Globorotalites michelinianus (d'Orbigny). Basov & Krasheninnikov, 1983,
pl. 8, figs. 7–9.

Dorothia filiformis (Berthelin) emend. Bartenstein, 1954
Plate 1, Figures 1, 2

Dorothia filiformis (Berthelin) Bartenstein, 1954, pl. 1, figs. 14–15.
Gaudryina filiformis Berthelin. Geroch & Nowak, 1984, pl. 2, figs. 8–9.

Ellipsoidina abbreviata Seguenza, 1859

Ellipsoidina abbreviata Seguenza, 1859, pl. 14, fig. 5. Bolli et al., 1994, fig.
37.35.

Gavelinella sp. 1
Plate 2, Figure 7

Gaudryina pyramidata Cushman, 1926

Gaudryina laevigata Franke var. *pyramidata* Cushman, 1926, pl. 16, fig. 8.
Gaudryina pyramidata Cushman. Ly & Kuhnt, 1994, pl. 2, fig. 14.

Gyroidinoides sp. ex gr. *nitidus* (Reuss, 1844)
Plate 2, Figure 12

Rotalina nitida Reuss, 1844, p.214
Rotalina nitida Reuss, 1845, pl. 8, figs. 52; pl. 12, figs. 8, 20.
Gyroidinoides crassa (d'Orbigny). Guérin, 1981, pl. 6, figs. 13–14.
Gyroidinoides nitidus (Reuss). Basov & Krasheninnikov, 1983, pl. 9, figs. 2–
3.

Gyroidinoides subangulatus (Plummer, 1927)
Plate 2, Figures 8, 11

Rotalia soldanii (d'Orbigny) var. *subangulata* Plummer, 1927, pl. 12, fig. 1.
Gyroidinoides subangulatus (Plummer). Ly & Kuhnt, 1994, pl. 5, fig. 6.

Hemirobulina bullata (Reuss, 1860)

Marginulina bullata Reuss, 1860, pl. 6, figs. 4–6.
Marginulina bullata Reuss. Scheibnerová, 1976, pl. 29, fig. 1. Bartenstein &
Bolli, 1986, pl. 5, figs. 17–18.

Laevidentalina catenula (Reuss, 1860)
Plate 1, Figure 11

Dentalina catenula Reuss, 1860, pl. 3, fig. 6.
Dentalina catenula Reuss. Basov & Krasheninnikov, 1983, pl. 6, fig. 8.
Laevidentalina catenula (Reuss). Bolli et al., 1994, fig. 26.12–13.

Laevidentalina soluta (Reuss, 1851)

Dentalina soluta Reuss, 1851, pl. 3, fig. 4a, b.
Dentalina soluta (Reuss). Weidich, 1990, pl. 39, figs. 11–12; pl. 40, fig. 7.

Lenticulina macrodisca (Reuss, 1863)

Cristellaria macrodisca Reuss, 1863 pl. 9, fig. 5a, b.
Lenticulina macrodisca (Reuss). Neagu, 1975, pl. 45, figs. 1–16, 20; pl. 47,
figs. 25–26. Weidich, 1990, pl. 21, figs. 1–2.

Lenticulina muensteri (Roemer, 1839)

Robulina muensteri Roemer, 1839, pl. 20, fig. 29a, b.
Lenticulina muensteri (Roemer). Bartenstein & Bolli, 1986, pl. 4, figs. 25–26.
Meyn & Vespermann, 1994, pl. 23, figs. 12–17; pl. 24, figs. 1–17.

Lenticulina rotulata (Lamarck, 1804)
Plate 1, Figure 8

Lenticulites rotulata Lamarck, 1804, p. 188.
Lenticulina rotulata (Lamarck). McNeil & Caldwell, 1981, pl. 16, fig. 14. Ly
& Kuhnt, 1994, pl. 3, fig. 10.

Lingulina taylorana Cushman, 1938

Lingulina taylorana Cushman, 1938, pl. 7, fig. 9. Bolli et al., 1994, fig. 27.16–
17.24.

Marginulinopsis lituola (Reuss, 1846)
Plate 1, Figure 13

Cristellaria lituola Reuss, 1846, pl. 24, fig. 47.
Marginulinopsis lituola (Reuss). Bolli et al., 1994, fig. 29.28–29.

Neobulimina subregularis (de Klasz, Magné, & Rérat, 1963)
Plate 3, Figure 4

Bulimina (*Neobulimina*?) de Klasz, Magné, & Rérat, 1963, pl. 1, fig. 9; pl. 2,
fig. 13.
Neobulimina subregularis (de Klasz, Magné, & Rérat). Petters, 1982, pl. 10,
figs. 28–29. Ly & Kuhnt, 1994, pl. 5, fig. 2.

Nodosaria aspera (Reuss, 1845)
Plate 1, Figure 12

Nodosaria aspera Reuss, 1845, 13. figs. 14–15.
Nodosaria aspera Reuss. Basov & Krasheninnikov, 1983, pl. 6, fig. 1.
Nodosaria aspera aspera Reuss. Bolli et al., 1994, fig. 26.30–31.

Nothia sp. ex gr. *excelsa* (Grzybowski) emend. Geroch & Kaminski, 1993
Plate 1, Figure 6

Nothia excelsa (Grzybowski) Kaminski & Geroch, 1993, pl. 1, figs. 2–6, 15.

Planularia complanata (Reuss, 1845)
Plate 1, Figure 9

Cristellaria complanata Reuss, 1845, pl. 13, fig. 54a, b.
Planularia complanata (Reuss). Magniez-Jannin, 1975, pl. 9, figs. 26–38 and
text-fig. 83. Weidich, 1990, pl. 40, figs. 13–14. Bolli et al., 1994, fig.
32.16.

Praebulimina fang (de Klasz, Magné, & Rérat, 1963)
Plate 3, Figure 12

Bulimina (*Praebulimina*?) *fang* de Klasz, Magné, & Rérat, 1963, pl. 1, fig. 6;
pl. 2, fig. 9.
Praebulimina fang (de Klasz, Magné, & Rérat). Tronchetti, 1981, pl. 3, figs.
5–8. Ly & Kuhnt, 1994, pl. 4, fig. 11.

Praebulimina proluxa longa (de Klasz, Magné, & Rérat, 1963)
Plate 3, Figure 5

Bulimina (*Praebulimina*?) *proluxa longa* de Klasz, Magné, & Rérat, 1963, pl.
1, fig. 7; pl. 2, figs. 10–11.

Praebulimina robusta (de Klasz, Magné, & Rérat, 1963)
Plate 3, Figure 7

Bulimina (*Praebulimina*?) *exigua robusta* de Klasz, Magné, & Rérat, 1963,
pl. 1, fig. 5; pl. 2, figs. 7–8.
Praebulimina robusta (de Klasz, Magné, & Rérat). Petters, 1982, pl. 11, figs.
23–24.

Praebulimina sp. 1
Plate 3, Figures 1, 2

Gabonita spinosa (de Klasz, Marie, & Meijer). Petters, 1982, pl. 7, figs. 23–
24.
Remarks: Our specimens are identical to those illustrated by Petters
(1982) as *Gabonita spinosa*.

Praebulimina sp. 2
Plate 3, Figure 3

Remarks: More elongated than *Praebulimina* sp. 1, also possess elongated, spined chambers.

Praebulimina sp. 3
Plate 3, Figure 6

Remarks: Short, stout triserial tests with no extension of chambers.

Psilocitharella recta (Reuss, 1863)

Vaginulina recta Reuss, 1863, pl. 2, figs. 14–15.
Vaginulina recta Reuss. Bartenstein & Bolli, 1986, pl. 6, figs. 7–8. Tronchetti & Grosheny, 1991, pl. 4, figs. 13–14.

Pyramidulina tetragona (Reuss, 1860)
Plate 1, Figure 3

Nodosaria tetragona Reuss, 1860, pl. 2, fig. 1.
Pyramidulina tetragona (Reuss). Bolli et al., 1994, fig. 27.14.

Pyrulina cylindroides (Roemer, 1838)
Plate 1, Figure 10

Polymorphina cylindroides Roemer, 1838, pl. 3, fig. 26a, b.
Pyrulina cylindroides (Roemer). McNeil & Caldwell, 1981, pl. 17, fig. 16.
Riegraf & Luterbacher, 1989, pl. 4, figs. 23–24.

Ramulina aculeata (d'Orbigny, 1840)
Plate 2, Figure 5

Nodosaria aculeata d'Orbigny, 1840, pl. 1, figs. 2–3.
Ramulina aculeata (d'Orbigny). Tronchetti & Grosheny, 1991, pl. 4, fig. 6.
Bolli et al., 1994, fig. 33.31.

Ramulina globotubulosa Cushman, 1938.
Plate 2, Figure 6

Ramulina globotubulosa Cushman, 1938., pl. 7, fig. 16.
Ramulina globotubulosa Cushman. Dam, 1950, pl. 4, fig. 1. Reicherter et al., 1994, pl. 7D, fig. L.

Saracenaria triangularis (d'Orbigny, 1840)

Cristellaria triangularis d'Orbigny, 1840, pl. 2, figs. 21–22.
Saracenaria triangularis (d'Orbigny). Moullade, 1984, pl. 3, fig. 1. Ly & Kuhnt, 1994, pl. 3, fig. 11.

Siphogenerinoides pygmaea de Klasz & Rérat, 1962
Plate 2, Figures 2, 3

Siphogenerinoides pygmaea de Klasz & Rérat, 1962, pl. 3, figs. 6–7.

Stilostomella alexanderi (Cushman, 1936)

Ellipsonodosaria alexanderi Cushman, 1936, pl. 9, figs. 6–9.
Stilostomella alexanderi (Cushman). Kaiho et al., 1993, pl. 7, fig. 10.

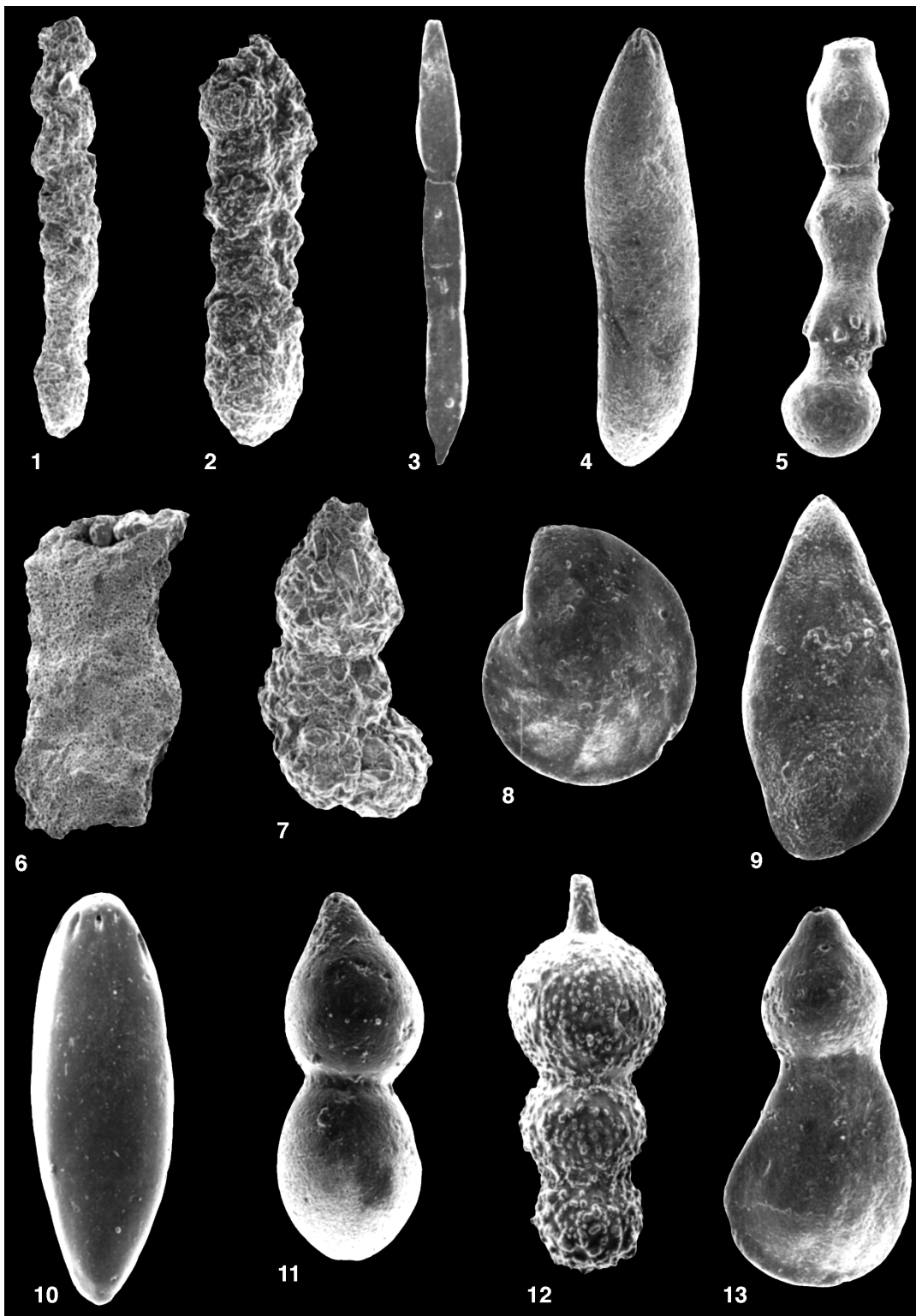


Plate 1. **1.** *Dorothia filiformis* (Berthelin) (60×), Sample 159-959D-67R-1, 140–144 cm. **2.** *Dorothia filiformis* (Berthelin) (60×), Sample 159-959D-66R-1, 21–25 cm. **3.** *Pyramidulina tetragona* (Reuss) (80×), Sample 159-959D-66R-4, 68–70 cm. **4.** *Astacolus parallelus* (Reuss) (110×), Sample 159-959D-66R-1, 21–25 cm. **5.** *Stilostomella* sp. (200×), Sample 159-959D-66R-4, 68–70 cm. **6.** *Nothia* ex gr. *excelsa* (Grzybowski) (50×), Sample 159-959D-67R-1, 140–144 cm. **7.** *Bulbobaculites* sp. (50×), Sample 159-959D-67R-1, 140–144 cm. **8.** *Lenticulina rotulata* (Lamarck) (60×), Sample 159-959D-66R-1, 21–25 cm. **9.** *Planularia complanata* (Reuss) (155×), Sample 159-959D-66R-3, 20–23 cm. **10.** *Pyrulina cylindroides* (Roemer) (120×), Sample 159-959D-66R-1, 68–71 cm. **11.** *Laevidentalina catenula* (Reuss) (100×), Sample 159-959D-66R-1, 68–71 cm. **12.** *Nodosaria aspera* (Reuss) (120×), Sample 159-959D-66R-1, 21–25 cm. **13.** *Margulinopsis lituola* (Reuss) (140×), Sample 159-959D-66R-1, 21–25 cm.

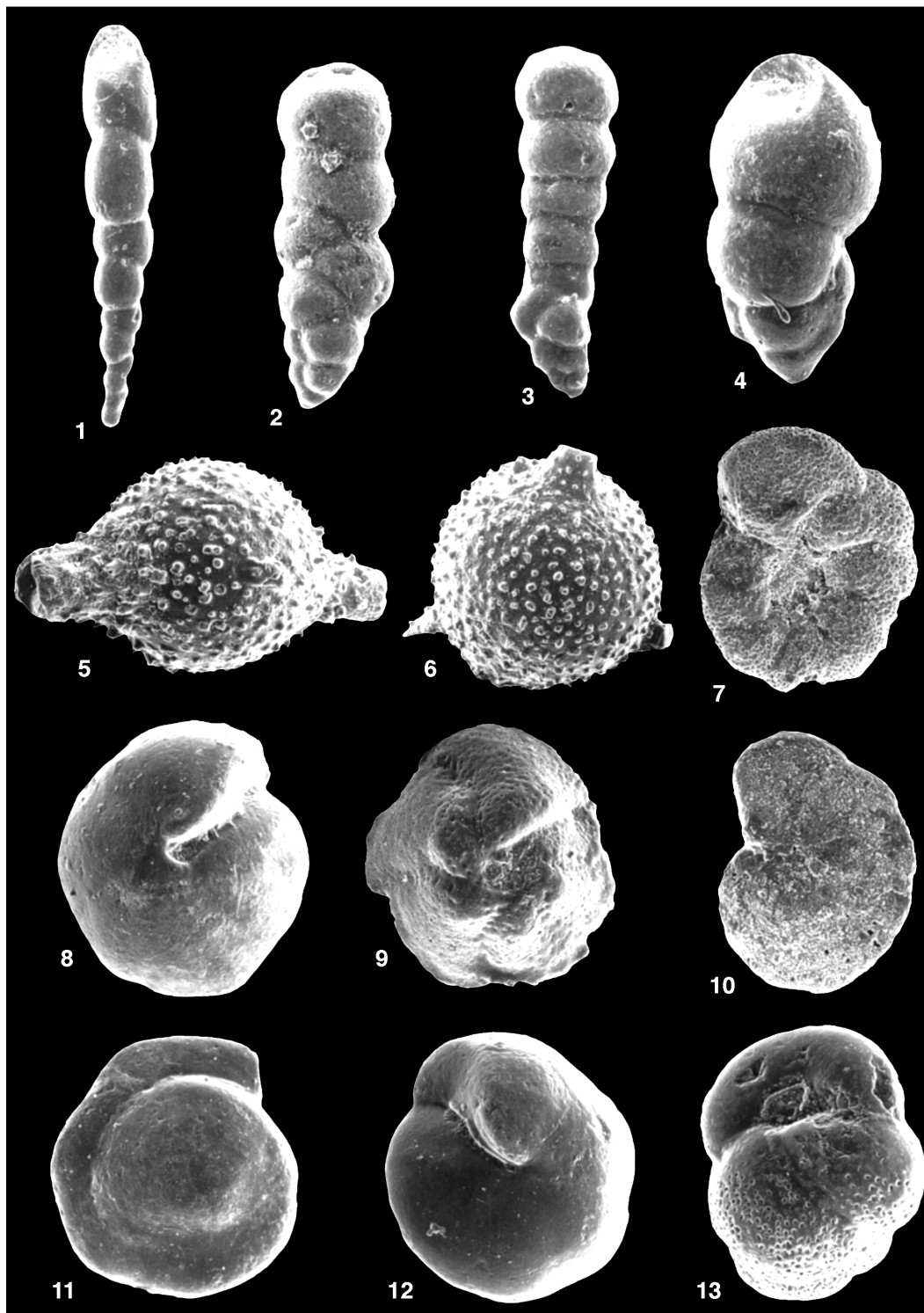


Plate 2. **1.** *Pleurostomella* sp. (140×), Sample 159-959D-66R-4, 68–70 cm. **2.** *Siphogenerinoides pygmaea* de Klasz and Rérat (245×), Sample 159-959D-66R-1, 68–71 cm. **3.** *Siphogenerinoides pygmaea* de Klasz and Rérat (180×), Sample 159-959D-66R-1, 68–71 cm. **4.** *Bandyella greatvalleyensis* (Trujillo) (120×), Sample 159-959D-66R-4, 21–23 cm. **5.** *Ramulina aculeata* (d’Orbigny) (200×), Sample 159-959D-66R-1, 68–71 cm. **6.** *Ramulina globotubulosa* Cushman (150×), Sample 159-959D-66R-1, 68–71 cm. **7.** *Gavelinella* sp. 1 (130×), Sample 159-959D-68R-1, 40–44 cm. **8.** *Gyroidinoides subangulatus* (Plummer) (120×), Sample 159-959D-66R-4, 21–23 cm. **9.** *Conorotalites michelinianus* (150×), Sample 159-959D-66R-1, 21–25 cm. **10.** *Gavelinella* sp. 1 (180×), Sample 159-959D-68R-1, 40–44 cm. **11.** *Gyroidinoides subangulatus* (Plummer) (130×), Sample 159-959D-66R-4, 21–23 cm. **12.** *Gyroidinoides* ex gr. *nitidus* (Reuss) (145×), Sample 159-959D-66R-1, 68–71 cm. **13.** *Buliminella* cf. *gabonica altispira* de Klasz, Magné, and Rérat (215×), Sample 159-959D-66R-5, 18–21 cm.

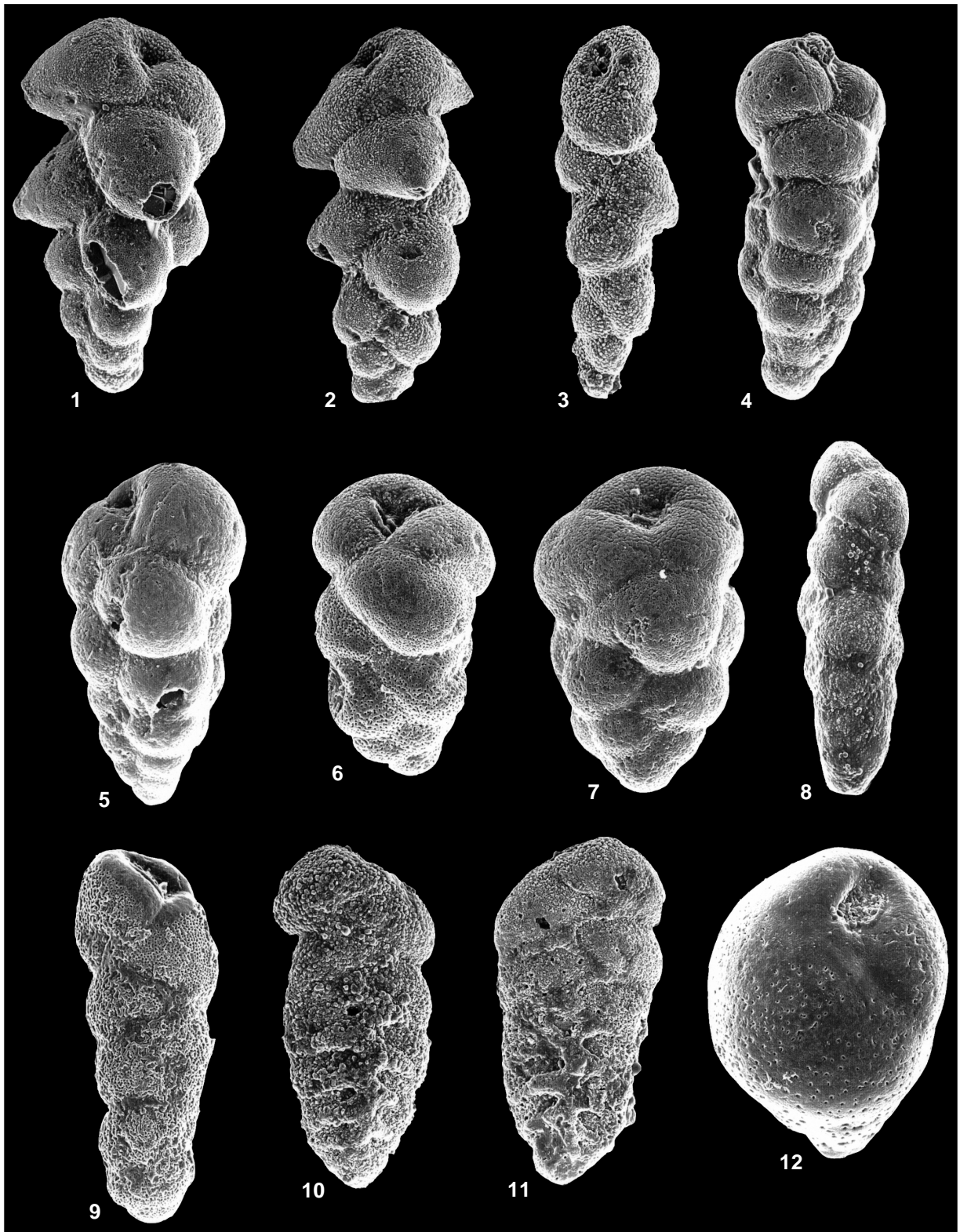


Plate 3. **1.** *Praebulimina* sp. 1 (200×), Sample 159-959D-686R-1, 40–44 cm. **2.** *Praebulimina* sp. 1 (200×), Sample 159-959D-686R-1, 40–44 cm. **3.** *Praebulimina* sp. 2 (200×), Sample 159-959D-68R-1, 40–44 cm. **4.** *Neobulimina subregularis* (de Klasz, Magné, and Rérat) (200×), Sample 159-959D-66R-1, 68–71 cm. **5.** *Praebulimina proluxa longa* (de Klasz, Magné, and Rérat) (240×), Sample 159-959D-66R-5, 18–21 cm. **6.** *Praebulimina* sp. 3 (210×), Sample 159-959D-68R-1, 40–44 cm. **7.** *Praebulimina robusta* (de Klasz, Magné, and Rérat) (240×), Sample 159-959D-66R-4, 68–70 cm. **8.** *Neobulimina subregularis* (de Klasz, Magné, and Rérat) (150×), Sample 159-959D-66R-3, 20–23 cm. **9.** *Bolivina* sp. (180×), Sample 159-959D-66R-1, 68–71 cm. **10.** *Bolivina anambra* Petters (230×), Sample 159-959D-68R-1, 40–44 cm. **11.** *Bolivina anambra* Petters (230×), Sample 159-959D-68R-1, 40–44 cm. **12.** *Praebulimina fang* (de Klasz, Magné, and Rérat) (230×), Sample 159-959D-66R-4, 68–70 cm.